ICANS-XV
15th Meeting of the International Collaboration on Advanced Neutron Sources
November 6-9, 2000
Tsukuba, Japan

11.4
Design of a TOF-SANS instrument for the Proposed Long Wavelength Target Station at the Spallation Neutron Source

P. Thiyagarajan[1*], K. Littrell[1], and P. A. Seeger[2]

[1]Intense Pulsed Neutron Source, Argonne National Laboratory, 9700 S. Cass Ave. Argonne, IL 60439, USA
[2]239 Loma del Escolar, Los Alamos, NM 87544, USA
[*]E-mail: thiyaga@anl.gov

Abstract

We have designed a versatile high-throughput SANS instrument [Broad Range Intense Multipurpose SANS (BRIMS)] for the proposed Long Wavelength Target Station at the SNS by using acceptance diagrams and the Los Alamos NISP Monte Carlo simulation package. This instrument has been fully optimized to take advantage of the 10 Hz source frequency (broad wavelength bandwidth) and the cold neutron spectrum from a tall coupled solid methane moderator (12 cm x 20 cm). BRIMS has been designed to produce data in a Q range spanning from 0.0025 to 0.7 $Å^{-1}$ in a single measurement by simultaneously using neutrons with wavelengths ranging from 1 to 14.5 Å in a time of flight mode. A supermirror guide and bender assembly is employed to separate and redirect the useful portion of the neutron spectrum with $\lambda > 1$ Å, by 2.3° away from the direct beam containing high energy neutrons and γ rays. The effects of various collimation choices on count rate, resolution and Q_{min} have been characterized using spherical particle and delta function scatterers. The overall performance of BRIMS has been compared with that of the best existing reactor-based SANS instrument D22 at ILL.

1. Introduction

Small angle neutron scattering (SANS) is being extensively used in the characterization of materials in the fields of polymers, biology, ceramics, metallurgy, porous materials, magnetism, etc. SANS has high sensitivity in the size range of 1 to 100 nm and thus can be used to probe complex hierarchical structures with distinct length scales. Although electron microscopy (EM) is a direct probe for the studies in this length scale it is impossible to use EM for *in situ* studies. SAXS has high sensitivity in the above length scale, but the different scattering cross-sections for elements available with neutrons provide unique advantages for the study of multi-component systems and magnetic materials. To probe the length scale of 1 to 100 nm one requires data in a wide Q ($4\pi\sin\theta/\lambda$, where 2θ is the scattering angle and λ is the wavelength of neutrons) range of 0.001 to 0.7 $Å^{-1}$. In our experience in running a productive SANS user program at the Intense Pulsed Neutron Source we have seen that more than 50% of the experiments take advantage of the wide Q range (0.004 – 0.8 $Å^{-1}$) available at the SAND instrument in a single measurement.

At present, the steady-state reactor based SANS instruments provide high resolution SANS data in the low Q (0.001 to 0.01 $Å^{-1}$) region, while the time-of-flight SANS instruments at the pulsed sources allow measurements in a wide Q region (0.01 to 0.8 $Å^{-1}$) with better resolution in a single measurement. Although the quality and density of the data in the low Q region (Q < 0.01 $Å^{-1}$) at the first generation time-of-flight SANS instruments such as SAND is less than adequate for the determination of radius of gyration (Rg) for larger particles (Rg > 100 Å) using conventional Guinier analysis, their capability in covering a wide Q range in a single measurement is a great advantage for parametric studies. For instance, to measure data in the Q range that is available at SAND (0.004 to 0.8 $Å^{-1}$), experiments have to be repeated 3 to 4 times at the reactor-based SANS instruments, by changing the geometry and the wavelength of the instrument. To sum up, the reactor-based SANS instruments are superior for measuring the scattering data in the low Q region while pulsed-source SANS instruments are excellent for measuring high quality data in a wide Q region in a single measurement.

What is needed in the near future for the wide SANS community is an hybrid SANS instrument that combines the best features of the reactor-based and TOF SANS instruments, capable of measuring data in a Q range of 0.001 to 0.7 $Å^{-1}$ in a single measurement. The time has come for this to become a reality with the advent of the proposed Long Wavelength Target Station (LWTS) at the Spallation Neutron Source (SNS) at Oak Ridge National Laboratory. This source will deliver a large flux of cold neutrons useful for SANS at a source frequency of 10 Hz (Fig. 1). The cold moderators are large and directly view the target, thus producing a large cold neutron flux for each proton pulse. This source will offer unprecedented opportunities to study time-dependent phenomena and systems at low concentration and low contrast levels. For example it will become possible to study pressure-dependent protein folding kinetics [1] and the temperature dependent phase separation and crystallization kinetics in polymers and metallic alloys using this instrument. At present, such biological experiments are done using time-resolved SAXS at synchrotrons where effects such as radiation induced aggregation is a big concern.

2. Neutron Spectrum at LWTS

Erik Iverson and Brad Micklich have carried out careful Monte Carlo simulations of the neutron spectrum expected from different solid methane moderators at LWTS. Fig. 1 shows the normalized neutron spectra for three of the cases studied. We plan to place BRIMS on the coupled slab moderator which provides the maximum flux for the neutrons useful for SANS applications (λ=1 to 15 Å). We would like to point out that all the simulations that will be described below were performed assuming the neutron spectrum from a decoupled solid methane wing moderator that is viewed by SAND and scaled for the LWTS slab moderator. At the time of this paper, the pulse shapes from the simulations for the cold solid methane slab moderator proposed for the long wavelength target station have not been parameterized for use with NISP. However, the proton beam power normalized average flux in the 1-15Å wavelength range for this moderator is 1.44 times larger than that of the IPNS C moderator. This factor has been included in our analysis.

3. Design Criteria

The scientific community would greatly benefit by a versatile SANS instrument that can

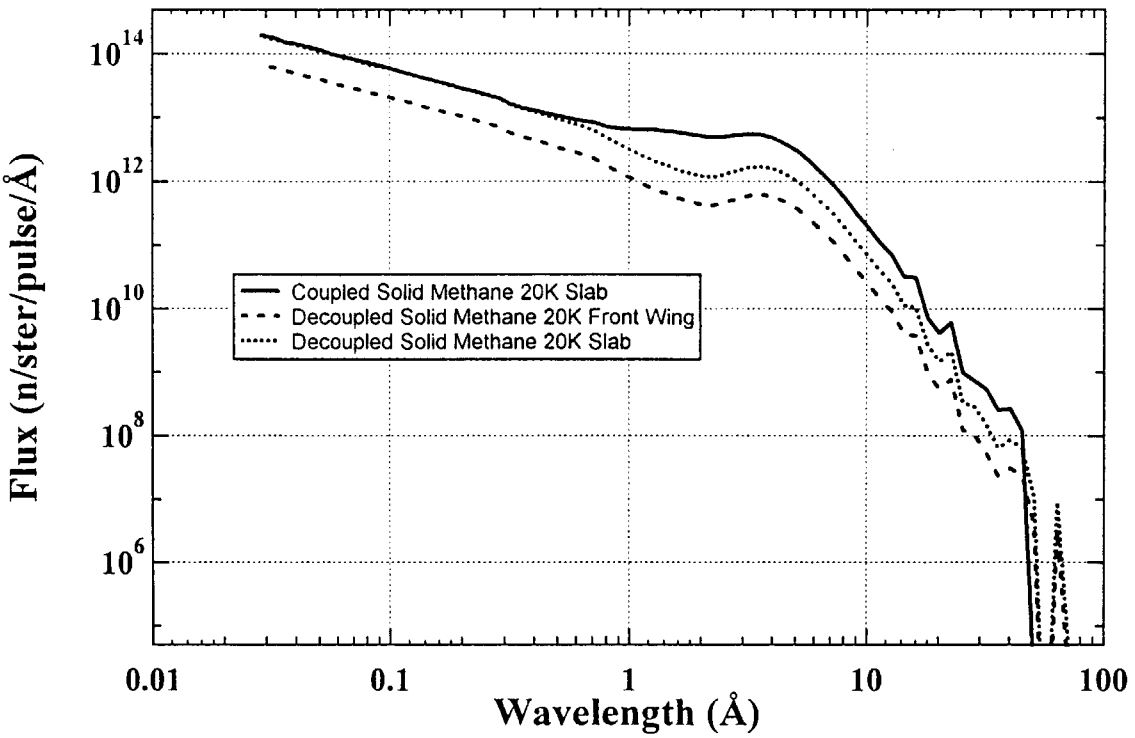

Fig.1. Simulated neutron spectra from the proposed moderators at the Long Wavelength Target Station at the SNS.

provide the highest flux and cover a Q range of 0.002 to 0.4 $Å^{-1}$ in a single measurement. This instrument is designed to meet such a need. Options should be available to extend the Q ranges on both ends by selecting the collimation and beam stop size as well as the position of the area detector. One important consideration in this design has to be to separate the neutrons useful for SANS (λ =1 to 15 Å) efficiently from the high-energy and γ ray components of the direct beam to reduce the background.

The Q_{min} and Q_{max} in this instrument are determined by

$$Q_{min} = 4\pi \sin \theta_{min}/\lambda_{max} \quad (1)$$

$$Q_{max} = 4\pi \sin \theta_{max}/\lambda_{min} \quad (2)$$

The available bandwidth ($\Delta\lambda$) or the maximum wavelength (λ_{max}) useful in a given frame can be calculated using

$$\Delta\lambda = \lambda_{max} = 3955/f\,L \quad (3)$$

where f is the repetition rate and L is the length of the instrument. While designing this instrument, we set the maximum length of the instrument to be 31 m with the sample being at the 23 m and the entrance aperture at 15 m from the source. The area detector can be placed either at 27 m (λ_{max}=14.6 Å) or at 31 m (λ_{max}=12.75 Å) from the source, each providing unique advantages in flux and Q resolution depending on the experiment. For example, the longer sample to detector distance gives slightly higher resolution and higher point density at

each Q while shorter sample to detector distance allows higher flux on sample and a broader Q range. Horizontally offsetting the detector will increase Q_{max} and improve the resolution and statistical quality of the data at middle and high Q regions. Since the multiple scattering effects vary as λ^2, we restrict the λ_{max} to be < 15 Å.

4. Instrument Layout

The schematic of BRIMS is shown in Figure 2. This instrument will be situated on the long wavelength target station wherein the neutrons are produced by bombarding a heavy metal target with 1 GeV proton pulses with 0.3 μs pulse width (FWHM) at 10 Hz. High energy neutrons thus generated will be thermalized by a 12 cm x 20 cm coupled solid methane moderator to produce a large cold neutron flux. Key features of this instrument are as follows: It will use a supermirror coated guide and bender assembly to separate the useful cold neutrons away from the fast neutrons and the γ rays so that neither the sample nor the area detector will view them. A space of 1.4 m space between beam bender and collimation is allocated for spectral filters or polarizer elements. It will provide a choice of various pinholes and multiplexed pinholes that can be selected by the user depending on the experimental requirements. It will employ a moveable, 100 x 100 cm^2 position sensitive area detector with small pixels and a high data rate. Frame definition choppers or mirror filters will be used to eliminate neutrons with wavelength greater than 15 Å. High angle bank detectors can be augmented to extend the Q_{max}. We describe the properties of individual components used in the simulations below.

5. Bender and Guide Assembly

The prompt neutron spectrum from the target and moderator system contains a large amount of fast neutrons and γ rays which must be prevented from entering the collimation system. Currently, four different techniques are in use to reduce or eliminate the fast neutrons at different pulsed neutron sources. The SANS instrument at the KENS pulsed source at KEK in

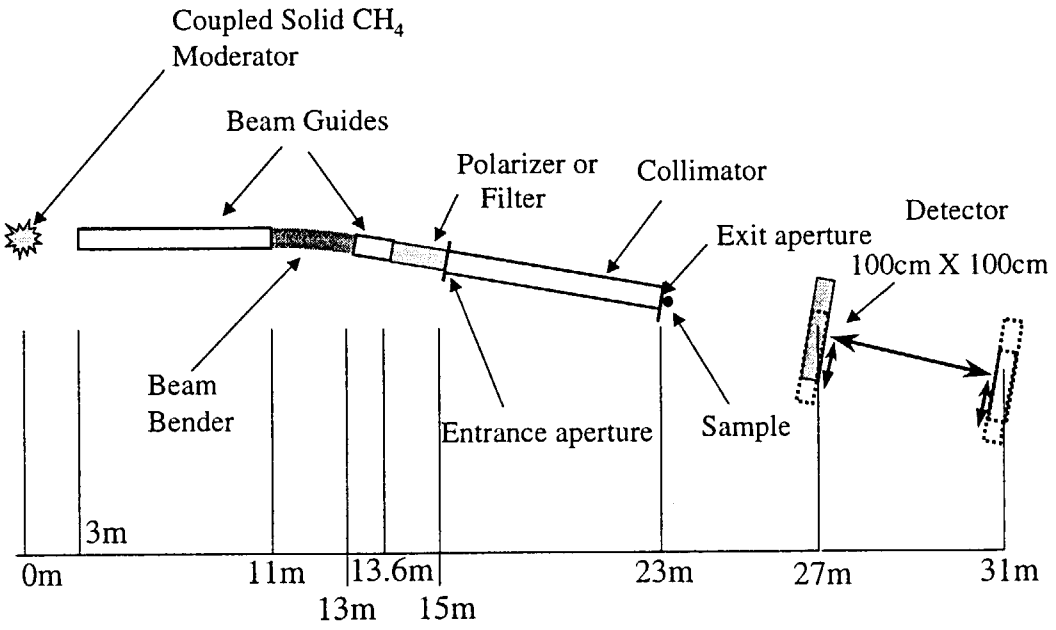

Fig.2. Schematic of the Broad Range Intense Multipurpose SANS instrument for the proposed Long Wavelength Target Station at SNS.

Japan uses a long reflecting bent neutron guide to make the detector out of sight of the source [2]. The LOQ instrument at the ISIS pulsed source in the UK [3] employs a beam bender (an array of short narrow curved guides placed side by side) for this purpose. The two SANS instruments at IPNS utilize cold MgO filters [4-6] and the LQD instrument at LANSCE [7] uses a T_0 chopper to attenuate the fast neutrons.

For BRIMS, we have chosen to use a guide and bender assembly to separate the cold neutrons from the direct beam so that the area detector is completely out of line-of-sight of the source. To improve the flux at short wavelengths, we have assumed the use of high index supermirrors to accept the short wavelength neutrons at higher angles. A 2 m long, 44.625 mm wide bender consisting of several 15 cm tall vertical blades follows the input snout. Each blade that gets inserted in the bender consists of a 0.2 mm SiO_2 substrate on which 3.5 μm thick m=3.5 supermirror (high angle reflectivity index =0.7) is coated on the reflecting side.

The critical wavelength for a curved guide or bender is defined as the wavelength for which a line tangent to the convex surface of the guide or bender channel intersects the concave surface at the critical angle for the guide mirror. Hence, the width w of each guide channel, given by

$$w = \frac{l}{2\theta_B}\left(m\lambda_C\gamma_C^{Ni}\right)^2, \tag{4}$$

where $\lambda_C = 1$ Å is the critical wavelength, l is the length of the curved guide or bender, θ_B is its bend angle, and $\gamma_C^{Ni} = 0.0017$ rad/Å determines the critical angle for natural nickel. Thus, for a given critical wavelength, the number of blades within the total width depends on the required bend angle. For example, a 11.95 mR bender has 15 channels while a 40 mR bender has 50 channels.

If the high energy neutron fraction of the neutron beam is to be eliminated as a radiological hazard and a background problem, there must be an additional 2m of heavy shielding material such as along line-of-sight through the entire bender system. Therefore, there may need to be straight snout sections of guide encased in heavy shielding before and/or after the bender itself. The length necessary is minimized if the lengths of the two snouts are the same. This minimum length l_S is given by

$$l_S = \frac{W}{\sin(\theta_B/2)} - \frac{l}{2\tan(\theta_B/2)}\left(\frac{1-\cos(\theta_B/2)}{\sin(\theta_B/2)}\right), \tag{5}$$

where W is the total width of the bender. For a 11.95 mrad bender of the width discussed, the 11m moderator to bender distance centers the bender between 8m snouts, allowing for a 3m radius exclusion zone around the moderator. In this configuration, the direct beam is minimally separated from the beam incident on the sample, with the required heavy shielding ending 2m upstream fron the sample position. The 8 m long input snout consists of two 20 cm tall vertical blades which are separated by 44.625 mm. The inner surfaces are coated with 5 μm thick m=3 supermirror (high angle reflectivity index=0.8). The entrance collimator slit and the polarizer are inside exit snout, which is assumed to be absorbing except for the first 0.6m where it is coated on its horizontal inner surfaces with 3.5 μm thick m=3.5 supermirror. For a 40 mrad bender, which completely avoids line-of-sight on the area detector, the entrance

and exit snouts are only required to be 1.75m in length each so that the radius for the heavy shielding can be as low as 10.5m. Thus, if the bender is shifted upstream along the beam path with the total length of the supermirror guide lining along the beam path constant, the polarizer and the collimation can be moved completely outside the heavy shielding with minimal effect on the flux on sample.

6. Collimation

BRIMS will have various choices of collimation that can be selected by the user to match the Q range and flux to the requirements of the experiment. Table 1 compiles the pinhole diameters for the collimation along with the geometrical parameters and the expected relative flux for each collimation geometry. The collimation system consists of two circular slits with the entrance slit at 15 m and the exit slit at 23 m from the source. Via computer control, various different size pinholes can be inserted at the entrance and sample slit positions and corresponding beam stop can be selected. Different combinations of pinholes and beam stops can be used depending on the required Q range and resolution.

7. Detector

A 100 cm x100 cm position sensitive small pixel, high data rate area detector will be used for typically used at the reactor-based instruments. This is the instrument geometry when the

Table 1
Instrument Settings considered for the full simulation of BRIMS

Entrance Aperture diameter (cm)	Sample aperture dia. (cm)	Beam stop Dia. (cm)	Entrance aperture to Sample aperture (m)	Sample to detector distance (m)	Relative Intensity from Acceptance diagrams	λ_{max} (Å)	Q_{min} ($Å^{-1}$)	Q_{max} With 1 Å neutrons ($Å^{-1}$)
4*	**1.33**	**4**	**8**	**4**	**1.00**	**14.5**	**0.00217**	**0.785**
3*	1.5	6	8	8	0.72	12.75	0.00185	0.393
3	**1**	**3**	**8**	**4**	**0.32**	**14.5**	**0.00163**	**0.785**
2*	***1***	***4***	***4***	***4***	***0.57***	***14.5***	***0.00217***	***0.785***
2	1	4	8	8	0.141	12.75	0.00123	0.393
2	**0.67**	**2**	**8**	**4**	**0.063**	**14.5**	**0.00108**	**0.785**
1.35	0.67	2.67	8	8	0.029	12.75	0.00082	0.393
1.35*	**0.45**	**1.35**	**8**	**4**	**0.0130**	**14.5**	**0.00073**	**0.785**
0.9	0.45	2	8	8	0.0058	12.75	0.00062	0.393

Parameters in bold and regular text correspond to 4m and 8m sample-to-detector distances, respectively. The parameters in bold italics were studied and found to be less preferable. The configurations marked with an (*) were extensively modeled using NISP.

detector is placed at 31 m position. In this geometry, a higher density of points can be measured at the lower values of Q , increasing the quality of the data at low Q and the number the scattering measurements. This detector will be mounted on rails so that it can be moved from 27 m to 31 m from the moderator as well as offset horizontally to increase the solid angle as required. The condition $L_1=L_2$, where L_1 is the entrance slit to sample slit distance and L_2 is the distance between the sample and the detector, is the symmetric case that is of points available for the Guinier analysis. In the asymmetric configuration, where $L_1=2L_2$, the instrument has higher flux and a wider Q range at the same Q_{min} as the symmetric configuration. The asymmetric configuration (detector at 27 m from the source) is the highest throughput mode for this instrument (see Table 1). The resolution of the instrument at a given value of Q is comparable for both configurations.

8. Supplementary Detector Banks

The BRIMS instrument can be augmented to extend the Q range up to 10 $Å^{-1}$ by the addition of supplementary detectors as has been done at the SAND instrument at IPNS [5] and the LOQ at ISIS [3]. These banks will be placed at angles as near to the transmitted beam as possible to minimize geometrical effects arising from the typical plane geometry of the sample for SANS. We plan to incorporate an high angle LPSD area bank to extend the Q_{max} to ~ 3 $Å^{-1}$ along with a back scattering detector cluster to extend to Q_{max} ~ 10 $Å^{-1}$. The detector sizes will be selected such that Q ranges from the supplementary detectors overlap substantially with each other as well as with that from the area detector, allowing for the data to be merged easily.

9. Polarizer

Space has been allocated for a multilayer-based or other transmission polarizer to polarize the neutron beam for the studies of magnetic materials. At the V4 instrument at BERII reactor of HMI, Berlin, a high efficiency spin flipper is being used for polarizing cold neutrons [8] with wide range of wavelengths above 4 Å. We believe that this technology will continue to improve and high efficiency polarizers and spin flippers for neutrons of nearly the full wavelength range of interest will be available when this instrument is ready to be built.

10. Frame Definition Mirror

The cold moderators will produce significant amounts of long wavelength neutrons that can arrive at the detector coincident with neutrons from subsequent pulses. Thus, their presence will cause frame overlap contamination. Hence, we plan to introduce a mirror whose critical angle is set to remove neutrons with $\lambda > 15$ Å to combat this problem. This can be installed upstream to the entrance aperture.

11. Methods of Instrument Performance Analysis

We used acceptance diagrams [9] to determine the appropriate collimation and beam stop dimensions to maximize the flux at the detector for our choice of Q range. Table 1 shows the settings that were considered along with the Q ranges and the fluxes at the detector. Evaluation of the instrument performance in terms of flux and Q resolution for various instrument parameters was carried out by using the Los Alamos NISP Monte Carlo package. This software package has a number of features that was required as per Kent Crawford's report [10]. This package utilizes correct physics modules for the interaction of neutrons with

a given component in the instrument. This allows for generating the geometry of the instrument including the position and orientation of the different components, surfaces, regions, and the materials involved in each. In addition, the Monte Carlo engine that moves neutrons between components and handles statistics also allows the saving of histories to identify the sources of problems. It is capable of realistically tracking neutrons through an instrument from moderator to detector and it simulates scattering from spherical particles of any size and delta function scatterers. Furthermore, this package handles the effects of gravitation, neutron polarization and multiple scattering. We believe that all these features are extremely important in the evaluation of the instrument performance. Since the LWTS spectrum for a slab modetrator was not available at the initial stages of this project we used the neutron spectrum (λ=1 to 14.5 Å) from the decoupled solid methane wing moderator viewed by SAND as the source for the BRIMS instrument evaluation. Prior to carrying out the simulation of BRIMS we validated the simulation results by simulating the SAND instrument and comparing the results with the experimental data.

In order to compare the performance of BRIMS with what is generally acknowledged as the World's flagship SANS instrument, D22 at ILL, France, we simulated the D22 instrument with the appropriate neutron guides and the actual neutron spectrum (published at www. Ill.fr). Upon our request Dr. Roland May, the instrument scientist of D22 kindly provided the following 3 settings that would be useful to cover a Q range of 0.001 to 0.5 $Å^{-1}$ at D22. The Q range of 0.001 to 0.012 $Å^{-1}$ can be measured using 18 Å neutrons and a sample-to-detector distance of 18 m and the Q range of 0.0052 to 0.063 $Å^{-1}$ can be covered using 7.5 Å neutrons and a sample-to-detector distance of 8 m. The high Q region 0.026 to 0.5 $Å^{-1}$ can be accessed with 7.5 Å neutrons and a sample-to-detector distance of 1.4m along with a detector offset of

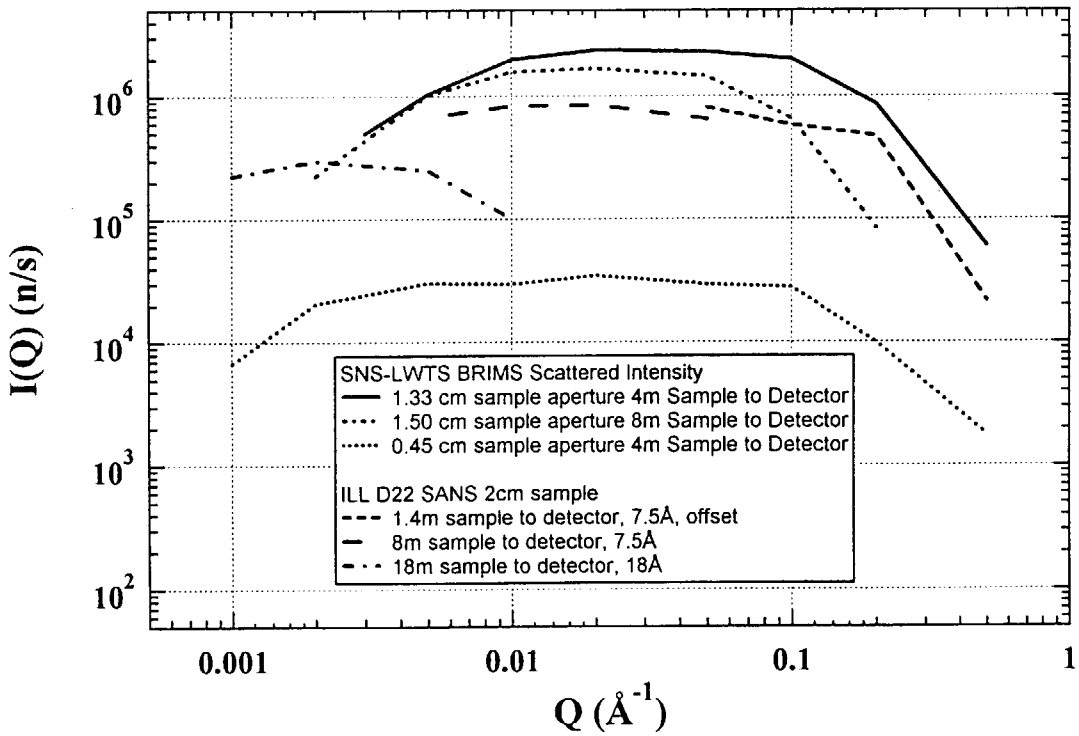

Fig.3. The normalized count rate at different Q values for BRIMS and D22 as obtained from the Monte Carlo simulations

0.39 m. We carried out simulations for these settings and compared the normalized scattered neutrons per second and the resolution in the whole Q range.

12. Results and Discussion

We have carried out our Monte Carlo simulations for BRIMS using the settings indicated in Table 1 assuming delta scatterers at Q = 0.002 $Å^{-1}$, 0.005 $Å^{-1}$, 0.01 $Å^{-1}$, 0.02 $Å^{-1}$, 0.05 $Å^{-1}$, 0.1 $Å^{-1}$, 0.2 $Å^{-1}$, 0.5 $Å^{-1}$ as well as spherical particles. The scattering from the delta function scatterers provide both the normalized intensity of scattered neutrons per second and the ΔQ at each Q value studied. We carried out similar calculations for the 3 settings for D22 described above. The normalized scattered neutron count rates for each Q for both BRIMS and D22 are shown in Fig.3. The normalization factor between the wing moderator viewed by SAND and the slab moderator at LWTS was determined by scaling for the size, proton power and the conversion efficiency offered by the slab moderator. It can be seen from Fig. 3 that at BRIMS the count rates are higher than that at D22. Furthermore, the data in a wide Q range is produced in a single measurement while it takes 3 settings at D22.

The simulation of the delta function scatterers at different Q values provides the resolution over the whole Q range. The solid lines in Fig. 4 correspond to BRIMS while the dotted lines correspond to the two sample-to-detector distances of 8 m and 1.4 m for D22. As expected, there exists a discontinuity in the ΔQ values for the D22, while it continuously varies for BRIMS. The gravitation effects for 18 Å neutrons with the18 m sample-to-detector distance were clearly observed in the simulations, where the beam drops about 7 cm from the direct view at the detector. The ΔQ values for this configuration is about half of that of BRIMS for

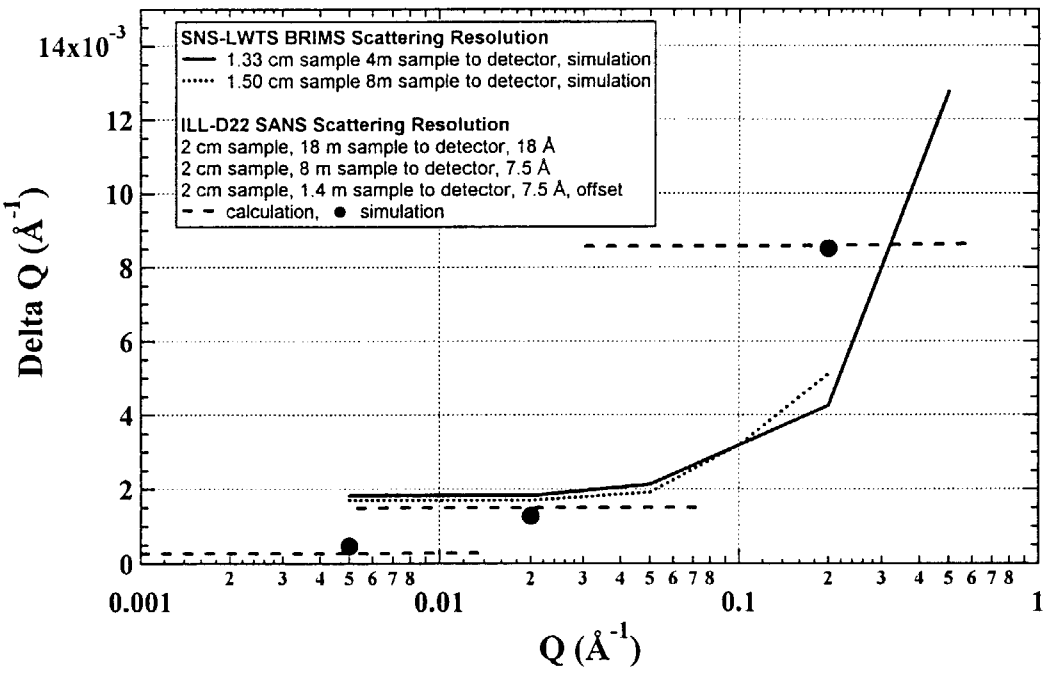

Fig. 4. ΔQ values obtained from the simulation using the delta function scatterers for BRIMS and D22. The points in the figure are those calculated using equation 6 which agree quite well with those obtained from the simulated data.

$Q < 0.002$ Å^{-1}. The lines in the figure are the ΔQ values calculated using Equation 6 [11] for the two instrument configurations.

$$(\Delta Q)^2 = \frac{1}{12}\left(\frac{2\pi}{\lambda}\right)^2\left[3\frac{R_1^2}{2L_1^2} + \frac{3}{2}R_2^2\left(\frac{1}{L_1^2}+\frac{1}{L_2^2}\right) + \frac{(\Delta R)^2}{L_2^2} + \frac{R^2}{L_2^2}\left(\frac{\Delta\lambda}{\lambda}\right)^2\right] \quad (6)$$

In Equation 6, L_1 is the entrance slit to sample slit distance and L_2 is the sample-to-detector distance, R_1 and R_2 are the radii of the entrance and sample slits and $\Delta\lambda/\lambda$ is the wavelength dispersion, R is the radius of the annulus and ΔR is the width. It is important to note in Fig. 4 that the calculated ΔQ values for D22 at the 3 settings agree quite well with those determined from the simulation with the delta function scatterers using NISP. Such agreement inspires confidence in the simulation results regarding both the flux of the scattered neutrons and the resolution for BRIMS. In fact this is one of the better ways to determine the relative flux and resolution of instruments which simultaneously employ multiple wavelengths.

13. Bender performance

In order to assess the effect of the bender and MgO filter on fast neutrons ($\lambda < 0.5$ Å) we have carried out simulations using the ISIS water moderator that has neutrons with a wavelength down to 0.1 Å . The 11 mR bender, the minimum to separate the useful portion of the spectrum from the direct beam, seems to cause a 15% reduction in transmitted intensity at useable wavelengths when compared to a straight guide. This bender permits significant amount of fast neutrons through the instrument. The preferred 40 mR (50 channel) bender, which completely avoids the line-of-sight of the source for the area detector regardless of in-line shielding, reduced the transmitted flux at useable wavelengths by 28%. Both benders outperformed the MgO filter [6] in both transmission of the useful flux and reduction of high energy neutron background.

14. Performance of Soller Collimators

We also simulated BRIMS using the conventional crossed pair of Soller collimators similar to those used at SAD [4] and SAND [5]. The Soller collimators considered here consist of a horizontal set (length = 1.177 m) with a total entrance and exit widths of 22.74 mm and 18.63 mm divided into 21 channels followed by a vertical set (length = 0.813 m) with a total entrance and exit widths of 20.36 mm and 17.25 mm divided into 23 channels. Fig. 5 shows the comparison of the scattered intensity with a small pinhole and a crossed pair of Soller collimators. For a given Q resolution the flux with Sollers is only marginally higher. Based on our experience with these type of Soller collimators the marginal gains in intensity are not advantageous as the surfaces in the Sollers do produce background that will compromise the low Q measurements. We strongly believe that the multiplexed small pinholes would prove more advantageous than crossed Soller collimators.

15. Summary

We have described the design of a versatile TOF-SANS instrument (BRIMS) for the proposed long wavelength target station at SNS designed using acceptance diagrams and evaluated using NISP Monte Carlo simulations. This instrument combines features from the best reactor-based and the pulsed source SANS instruments. Our simulations show that the BRIMS in its high-throughput configuration (entry #1 in Table 1) should have a few times

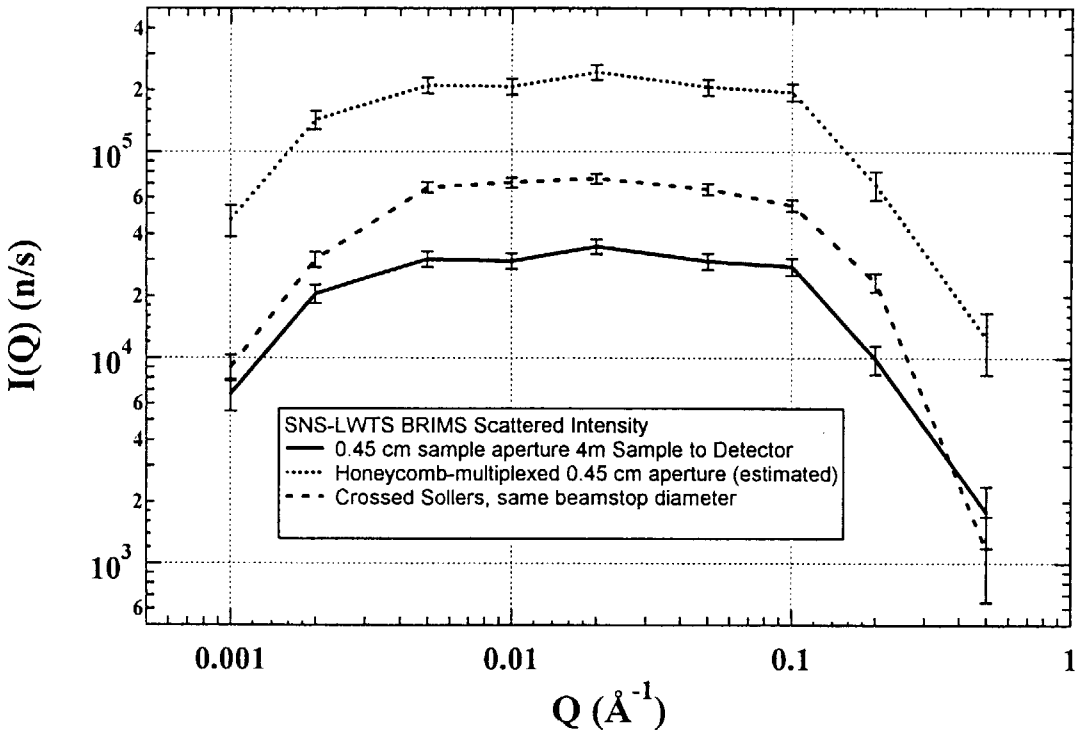

Fig.5. Comparison of the scattered neutrons/s determined from the simulations for the small pinhole with the crossed pair of Soller collimators. The curve for the multiplexed pinholes has been estimated using the results from the simulation for the single pinhole.

higher scattered intensity and comparable resolution when compared to the D22 at ILL. In the symmetric configuration it will produce high resolution data in the low Q region just like the reactor instruments. The D22 is noticeably better than BRIMS in terms of flux and resolution only at $Q < 0.002$ Å^{-1} when it employs 18 Å neutrons at a sample to detector distance of 18 m. In our estimate, using honeycomb or bottle-case type multiplexed narrow pinholes on BRIMS will narrow that gap substantially with regard to flux in that low Q region although a penalty in resolution will inevitably remain due to a shorter instrument and shorter operating wavelength (see equation 6).

Acknowledgments

This work has benefited from the use of IPNS, supported by the U.S. Department of Energy, BES-Materials Science, under contract W-31-109-ENG-38 to the University of Chicago and NSF grant # DMR-0073038. We thank Dr. Roland May, ILL, Grenoble, France for providing expert information on D22 that was useful to compare the instrument performances. We are grateful to Dr. John Ankner, SNS, for providing the Excel macros to calculate the acceptance diagrams and Ed Lang, IPNS for drawing the schematic of the BRIMS instrument.

References

[1] J. Woenkhaus, R. Kohling, P. Thiyagarajan, K. Littrell, S. Seifert, C.A. Royer & R. Winter (2000). Biophysical J. (In Press).

[2] Y. Ishikawa, M. Furusaka, N. Nimura, M. Arai & K. Hasegawa (1986) J. Appl. Cryst. 19, 229-242.

[3] R.K. Heenan & S.M. King, Proc. International Seminar on Structural Investigations at Pulsed Neutron Sources, Dubna, (1993) 176-184.

[4] P. Thiyagarajan, J.E. Epperson, R.K. Crawford, J.M. Carpenter, T.E. Klippert, & D.G. Wozniak (1997) J. Appl. Cryst. 30, 280-293.

[5] P. Thiyagarajan, V. Urban, K. Littrell, C. Ku, D.G. Wozniak, H. Belch, R. Vitt, J. Toeller, D. Leach, J.R. Haumann, G.E. Ostrowski, L.L. Donley, J. Hammonds, J.M. Carpenter & R.K. Crawford (1998a), Proceedings of ICANS XIV - The XIV Meeting of the ICANS, June 14-19, 1998, Starved Rock Lodge, Utica, Illinois, edited by J.M. Carpenter & C. Tobin, Volume **2**, 864-878. Springfield, VA: National Technical Information Service.

[6] P. Thiyagarajan, R.K. Crawford & D.F.R. Mildner (1998b) J. Appl. Cryst. 31, 835-840.

[7] P.A. Seeger, R.P. Hjelm, & M.J. Nutter (1990) Mol Cryst. Liq. Cryst 18A, 101-117.

[8] Th. Keller, A. Wiedenmann, Th. Krist, F. Mezei (1999). Nuc Inst. Methods (In Press).

[9] J.M. Carpenter & D.F.R. Mildner (1982). Nucl. Inst. Meth. A 196, 341.

[10] R.K. Crawford, (1998a), Proceedings of ICANS XIV - The XIV Meeting of the ICANS, June 14-19, 1998, Starved Rock Lodge, Utica, Illinois, edited by J.M. Carpenter & C. Tobin, Volume **2**, 881-883. Springfield, VA: National Technical Information Service.

[11] D.F.R. Mildner & J.M. Carpenter (1984). J. Appl. Cryst., **17**, 249-256.